

UNCLASSIFIED

RM No. L7J03

Copy No.

~~RESTRICTED~~**NACA****RESEARCH MEMORANDUM****24 DEC 1947**

INVESTIGATION OF PRESSURE DISTRIBUTION OVER AN EXTENDED
LEADING-EDGE FLAP ON A 42° SWEPTBACK WING

By

D. William Conner and Gerald V. Foster

Langley Memorial Aeronautical Laboratory
Langley Field, Va.**CLASSIFICATION CANCELLED**

CLASSIFIED DOCUMENT

This document contains classified information affecting the National Defense of the United States within the meaning of the Espionage Act, USC 50-31 and 32. The transmission or the revelation of its contents in any manner to an unauthorized person is prohibited by law. Information so classified may be imparted only to persons in the military and naval services of the United States, approved civilian officers and employees of the Federal Government who have a legitimate interest therein, and to United States citizens of known loyalty and discretion who of necessity must be informed thereof.

J. W. Crawley Date *12/14/53*
EO 10501
H-1-15-54 See *2000*
R72162

**NATIONAL ADVISORY COMMITTEE
FOR AERONAUTICS**

WASHINGTON

December 19, 1947

UNCLASSIFIED**NACA LIBRARY**LANGLEY MEMORIAL AERONAUTICAL
LABORATORY
Langley Field, Va.~~RESTRICTED~~



NATIONAL ADVISORY COMMITTEE FOR AERONAUTICS

RESEARCH MEMORANDUM

INVESTIGATION OF PRESSURE DISTRIBUTION OVER AN EXTENDED
LEADING-EDGE FLAP ON A 42° SWEEPBACK WING

By D. William Comer and Gerald V. Foster

SUMMARY

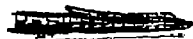
The pressure distribution over a leading-edge flap has been investigated in the Langley 19-foot pressure tunnel. The model was composed of a 42° sweptback wing of NACA 64-series sections attached to a fuselage in a high-wing position with deflected half-span split flaps and outboard extended leading-edge flaps. Measurements of pressure over the leading-edge flap were obtained through an angle-of-attack range at a Reynolds number and Mach number of 5,120,000 and 0.11, respectively. Some aerodynamic characteristics of the complete model were obtained at Reynolds number and Mach number of 6,840,000 and 0.14, respectively.

The results indicate that the flap normal-force coefficient increased almost linearly with angle of attack to a maximum value of 3.25. The maximum section normal-force coefficient was located about 30 percent of the flap span outboard of the inboard end and had a value of 3.75. Peak negative pressures built up at the flap leading edge as the angle of attack was increased and caused the chordwise location of flap center of pressure to be moved forward. In the high angle-of-attack range the center of pressure ranged between 49 and 55 percent of the flap chord.

INTRODUCTION

The investigation reported in reference 1 indicated that the inherently low maximum lift and poor longitudinal stability near the stall of swept wings can be greatly improved by the use of suitable leading-edge flaps. The design application of leading-edge flaps requires a knowledge of the flap loads in three-dimensional flow. Pressure-distribution measurements have, therefore, been made over a leading-edge flap for one of the more satisfactory combinations reported in reference 1 and the results are presented herein.

The 42° sweptback wing mounted on a fuselage in a high-wing arrangement had half-span split flaps and outboard extended leading-edge flaps. Both force measurements for the complete configuration



UNCLASSIFIED

and leading-edge-flap pressure measurements were obtained through the lift range at high values of Reynolds number and at values of Mach number corresponding approximately to take-off or landing conditions.

COEFFICIENTS AND SYMBOLS

The coefficients and symbols used herein are as follows:

α angle of attack of wing chord line

C_L lift coefficient (Lift/ qS)

C_D drag coefficient (Drag/ qS)

C_m pitching-moment coefficient referred to quarter-chord point of mean aerodynamic chord (Moment/ $qS\bar{c}$)

c_n section normal-force coefficient of leading-edge

$$\text{flap} \left(\int_0^1 \frac{p}{q} d \left(\frac{x}{c_f} \right) \right)$$

C_{N_f} normal-force coefficient of complete leading-edge

$$\text{flap} \left(\int_0^1 c_n d \left(\frac{y_f}{b_f} \right) \right)$$

c_{h_f} section hinge-moment coefficient of leading-edge flap (about

$$\text{trailing-edge point of flap chord}) \left(\int_0^1 \frac{p}{q} x d \left(\frac{x}{c_f} \right) \right)$$

C_{h_f} hinge-moment coefficient of leading-edge flap (about trailing

$$\text{edge of flap}) \left(\int_0^1 \bar{c}_{h_f} d \left(\frac{y_f}{b_f} \right) \right)$$

c.p. center of pressure of leading-edge flap in percent of flap chord

$$\text{measured from leading edge of flap} \left(100 - 100 \frac{c_{h_f}}{c_n} \right)$$

R Reynolds number (based upon wing mean aerodynamic chord)

S wing area (area of basic wing without flaps or fuselage)

q	free-stream dynamic pressure
\bar{c}	wing mean aerodynamic chord
p	local pressure minus free-stream static pressure
y_f	distance measured along span of leading-edge flap
b_f	leading-edge flap span
x	distance measured along chord of leading-edge flap
c_f	leading-edge flap chord measured perpendicular to flap leading edge

MODEL

The model used in the present tests is one previously used in the investigation reported in reference 1. The model configuration during these tests consisted of the high-wing-fuselage combination, half-span split flaps deflected 60° , and constant-chord leading-edge flaps. (See fig. 1.)

The leading-edge flaps henceforth referred to as the flaps, extended over a distance equal to 57.5 percent of the wing semispan with the inboard end of the flaps located at 40 percent of the wing semispan. As measured in a plane perpendicular to the wing quarter-chord line, a line connecting the leading edge of the wing with the center of the flap-nose radius had a 50° incidence with the wing chord. (See fig. 1.) The flap chord used in presenting pressure data was taken as the line connecting leading and trailing edges of the flap. (See fig. 2.) Orifices were installed in the right-hand flap at five spanwise stations. At each station and perpendicular to the flap leading edge, a row of nine orifices was set flush with the surface on the leading edge and upper surface of the flap. In addition, to measure the static pressure of the lower surface, two tubes were installed at the inboard, middle, and outboard stations. These orifices were not flush with the surface but any error in pressure measurement was believed to be small because the velocity at these orifices was extremely small. The spanwise location of the stations and chordwise location of the orifices for each station are shown in figure 2. The connecting leads for the orifices were fastened on the under surface of the flap behind the flap nose. Between the first and second row of orifices, the leads followed the wing lower surface in a streamwise direction back to the model support. Any disturbances resulting from the tube installation were believed to be small.

TESTS

Tests were made in the Langley 19-foot pressure tunnel with air compressed to approximately 33 pounds per square inch absolute. Pressures over the flap were measured on a multiple-tube manometer and recorded photographically for angles of attack of 6.8° , 11.1° , 15.3° , 18.5° , and 21.6° at a Reynolds number of 5,120,000 and a Mach number of 0.11. Measurements of lift, drag, and pitching moment of the complete model were made through a range of angle of attack of -4° through maximum lift at a Reynolds number of 6,840,000 and a Mach number of 0.14. The force measurements were obtained with the connector tubing removed from the model.

RESULTS AND DISCUSSION

The lift, drag, and pitching-moment characteristics are presented in figure 3. The ticked symbols indicate points at which flap pressure-distribution measurements were obtained. The chordwise variation of the pressure over the flap is presented in figure 4 at each spanwise station for the various angles of attack. Pressure coefficients obtained along the lower surface were faired point to point and no attempt was made to reach stagnation pressure ($\frac{p}{q} = 1.0$) since the effect on the force coefficient would be negligible. The dotted portions of the curves are interpolations (needed for integration) based on the existing data. At low angles of attack the peak negative pressures occurred near the flap trailing edge but as the angle of attack increased a peak pressure built up rapidly at the leading edge, especially near the inboard end of the flap. The maximum negative pressure coefficient of -6.4 was obtained at the station $\frac{y_f}{b_f} = 0.29$ at the highest angle of attack of the tests. The chordwise center of pressure which was located rather far back at low angles of attack moved toward the leading edge as the angle of attack was increased. (See fig. 4.) In the high angle-of-attack range it varied between 49 and 55 percent of the flap chord behind the flap leading edge, depending on the spanwise station.

The pressure-distribution curves were integrated to obtain the section normal-force coefficients and section moment coefficients about the assumed hinge location at the trailing edge of the flap. The chordwise-force coefficient was determined for a representative station and found to be about 1 percent of the normal-force coefficient; therefore, in determining the flap moment coefficients only the normal-force coefficient was used. The spanwise variation of the section coefficients is presented in figure 5. Throughout the lift range the maximum values of c_n and c_{h_f} occurred over the inboard 30 percent

of the flap span. These values dropped off gradually across the span at moderate and high angles of attack. As the angle of attack was increased above 15° the values of both c_n and c_{h_f} for the inboard station of the flap showed only a slight increase followed by a decrease. This was probably associated with the wing stall which was shown in reference 1 to start immediately behind the inboard end of flap.

The spanwise variation of the section coefficients was integrated to determine the total normal-force coefficient and flap moment coefficient; the variation of these values with angle of attack is presented in figure 6. The variation indicates a continuous increase of normal-force coefficient with angle of attack, though the slope of the curves decreased slightly above an angle of attack of 14° . The maximum value of C_{N_f} obtained was 3.25 which was about 87 percent of the maximum value of c_n obtained for the same angle of attack.

CONCLUDING REMARKS

The results of an investigation of the pressure distribution over a leading-edge flap on a sweptback wing indicate that the flap normal-force coefficient increased almost linearly with angle of attack, while the maximum section normal-force coefficient occurred outboard about 30 percent of the flap span from the inboard end. Peak negative pressures built up at the flap leading edge as the angle of attack was increased and caused the chordwise location of the center of pressure to move ahead to near the midchord point of the flap at high angles of attack.

Langley Memorial Aeronautical Laboratory
National Advisory Committee for Aeronautics
Langley Field, Va.

REFERENCE

1. Graham, Robert R., and Conner, D. William: Investigation of High-Lift and Stall-Control Devices on an NACA 64-Series 42° Sweptback Wing with and without Fuselage. NACA RM No. L7G09, 1947.

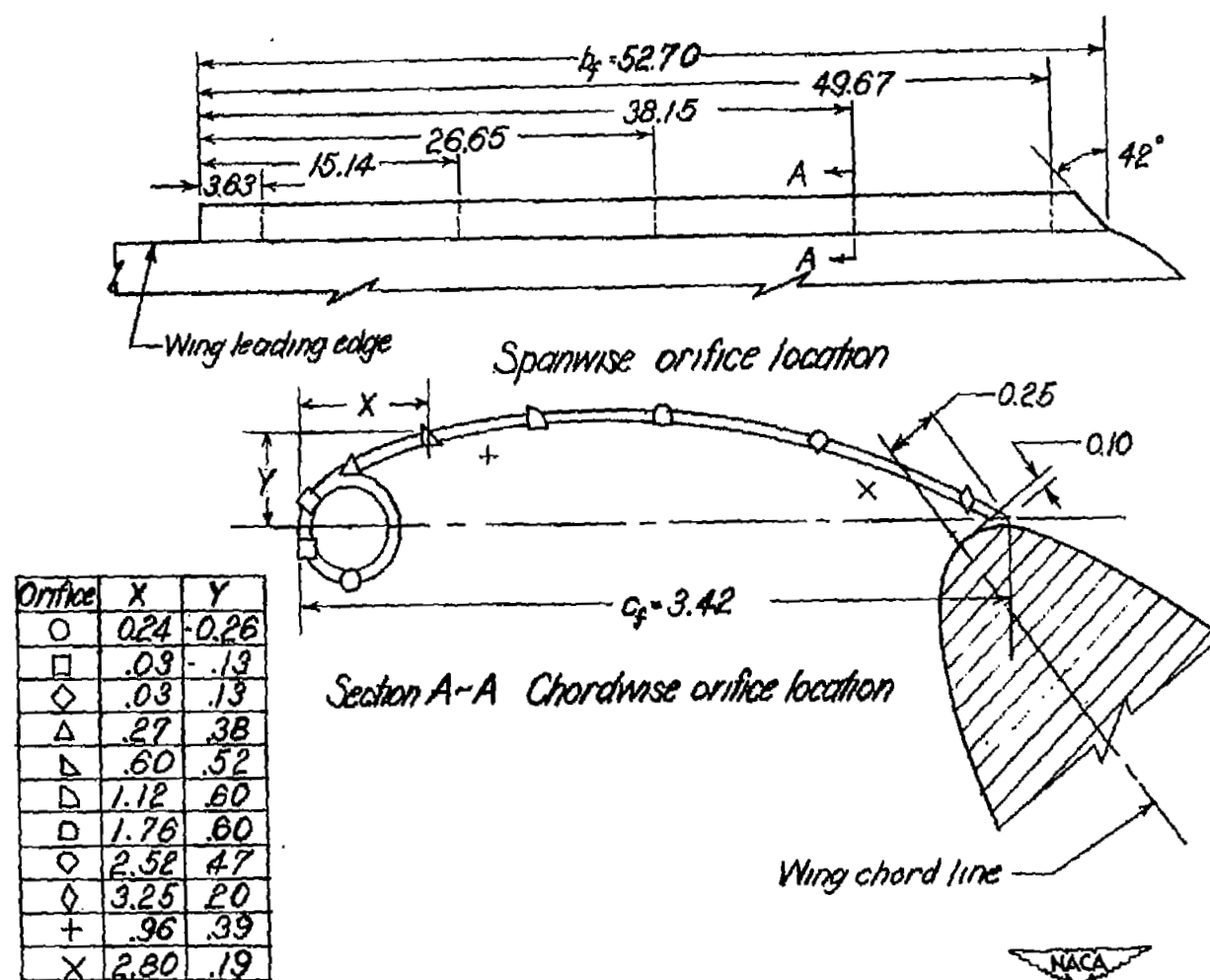


Figure 2.- Location of orifices on leading-edge flap. (All dimensions in inches)

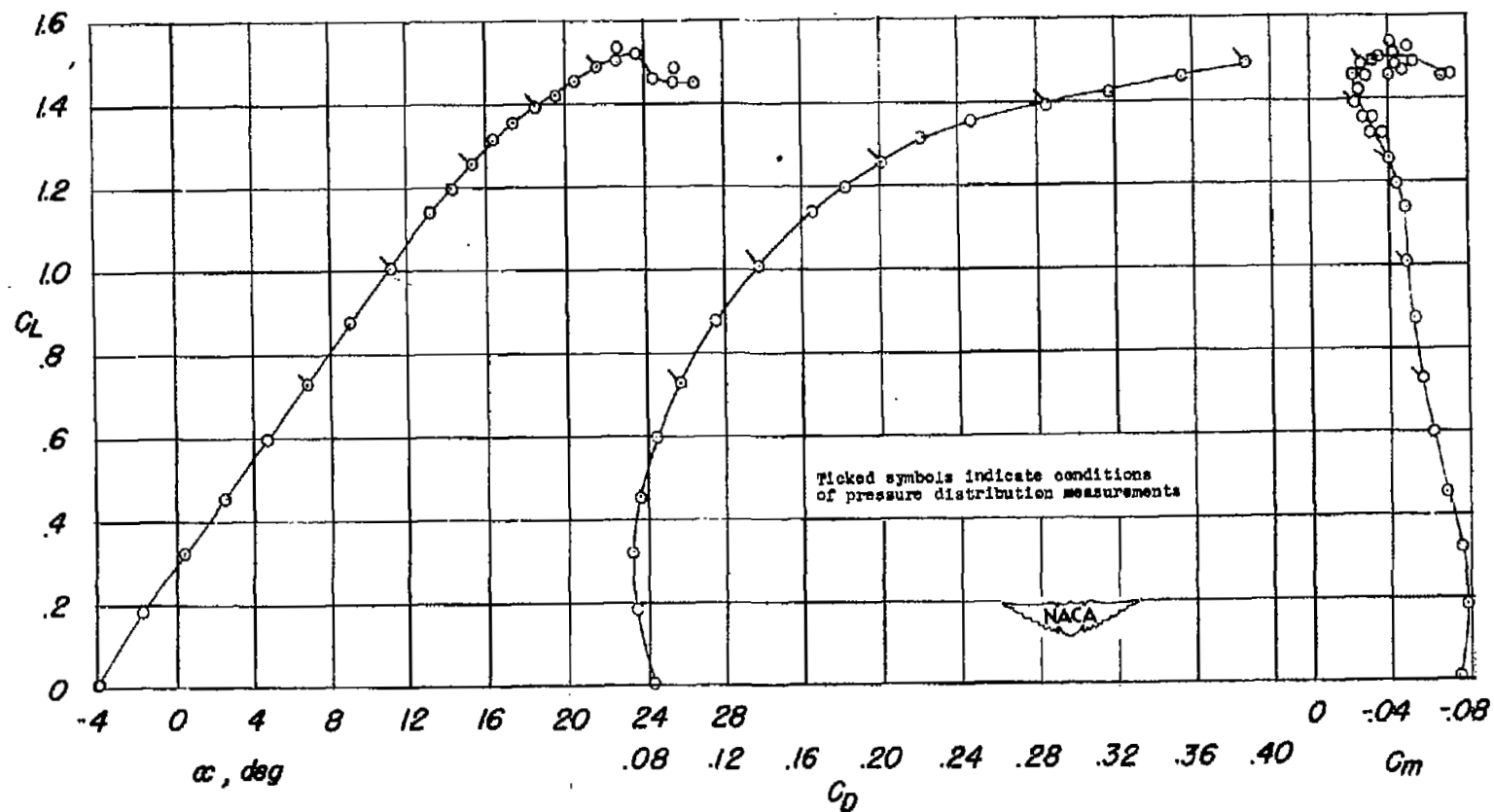


Figure 3.- Aerodynamic characteristics of 42° sweptback wing with fuselage on. Leading-edge flaps and normal split flaps. $R = 6,840,000$.

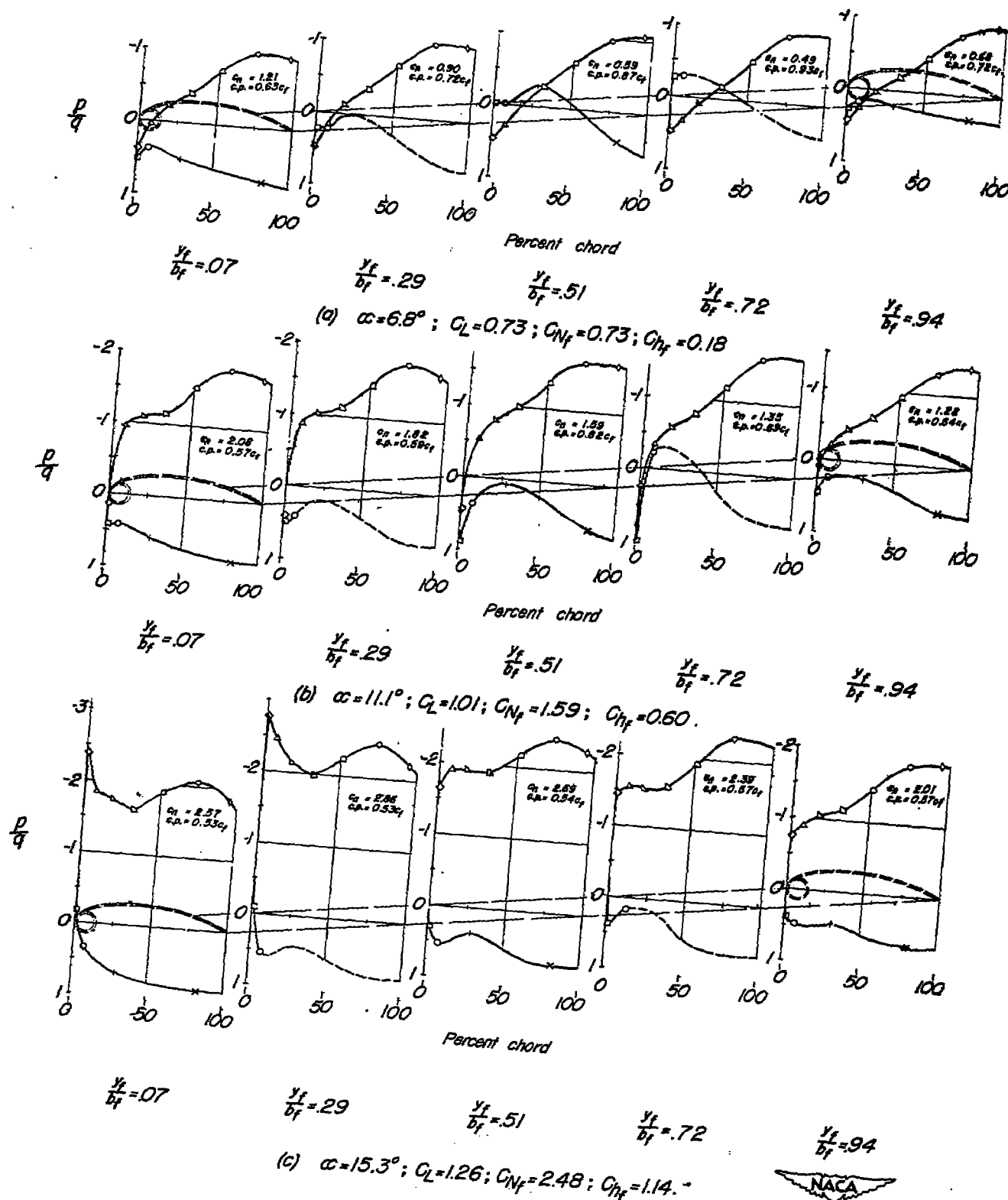
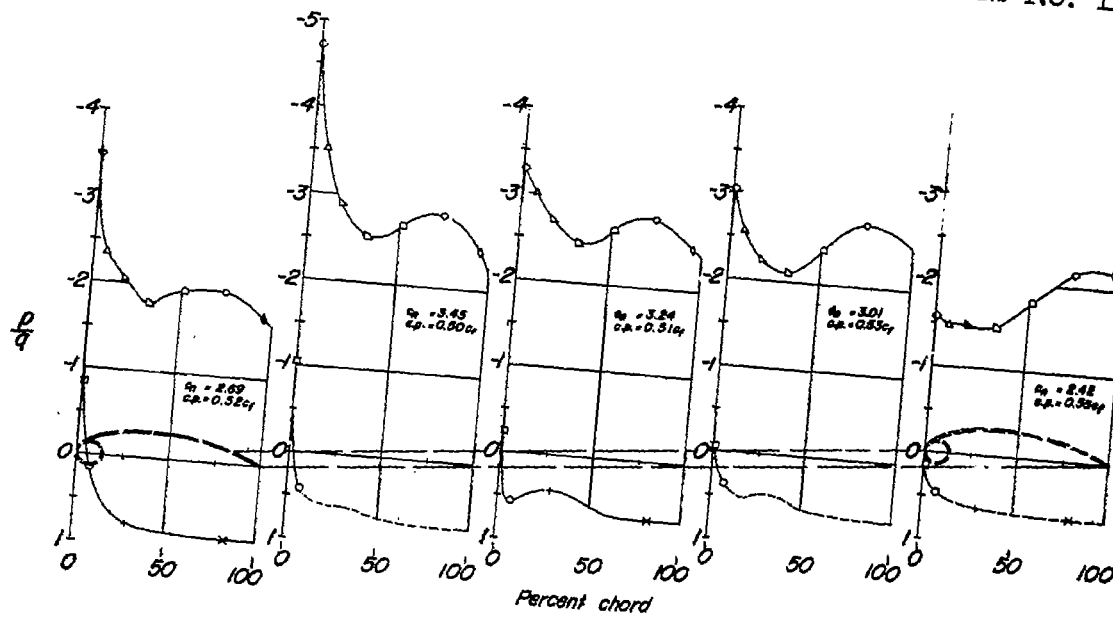


Figure 4.—Pressure distribution over a leading-edge flap for several angles of attack, $R = 5,120,000$.



$$\frac{y_f}{b_f} = 0.07$$

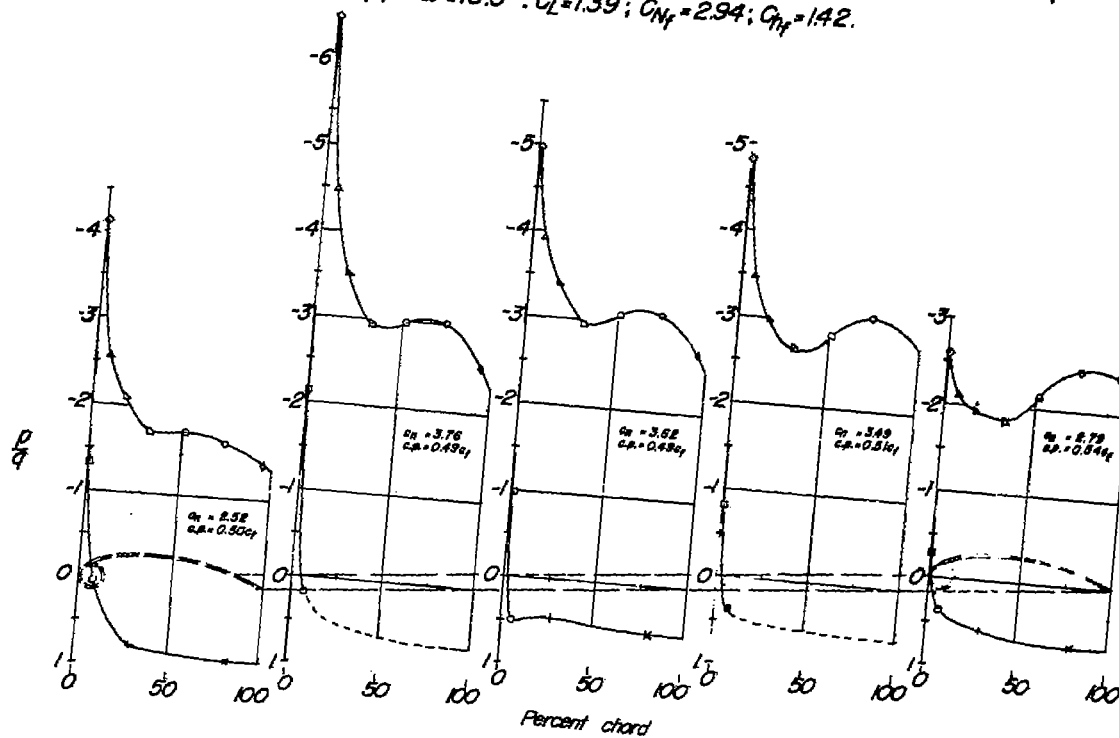
$$\frac{y_f}{b_f} = 0.29$$

$$\frac{y_f}{b_f} = 0.51$$

$$\frac{y_f}{b_f} = 0.72$$

$$\frac{y_f}{b_f} = 0.94$$

$$(d) \alpha = 18.5^\circ; C_L = 1.39; C_{N_f} = 2.94; C_{H_f} = 1.42.$$



$$\frac{y_f}{b_f} = 0.07$$

$$\frac{y_f}{b_f} = 0.29$$

$$\frac{y_f}{b_f} = 0.51$$

$$\frac{y_f}{b_f} = 0.72$$

$$\frac{y_f}{b_f} = 0.94$$

$$(e) \alpha = 21.6^\circ; C_L = 1.49; C_{N_f} = 3.24; C_{H_f} = 1.62.$$



Figure 4. — Concluded.

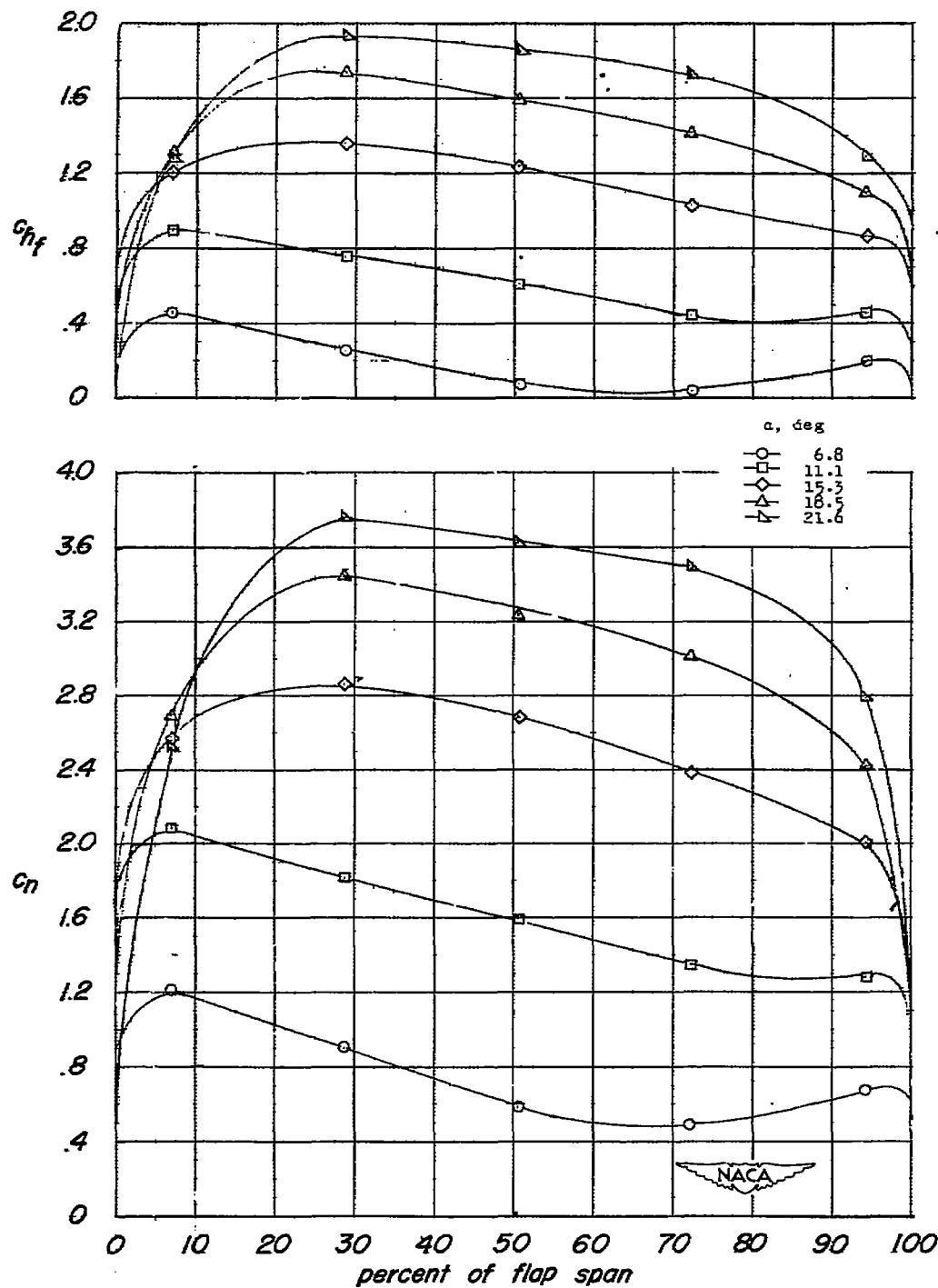


Figure 5.- Variation of flap normal-force coefficient and flap moment coefficient with angle of attack.

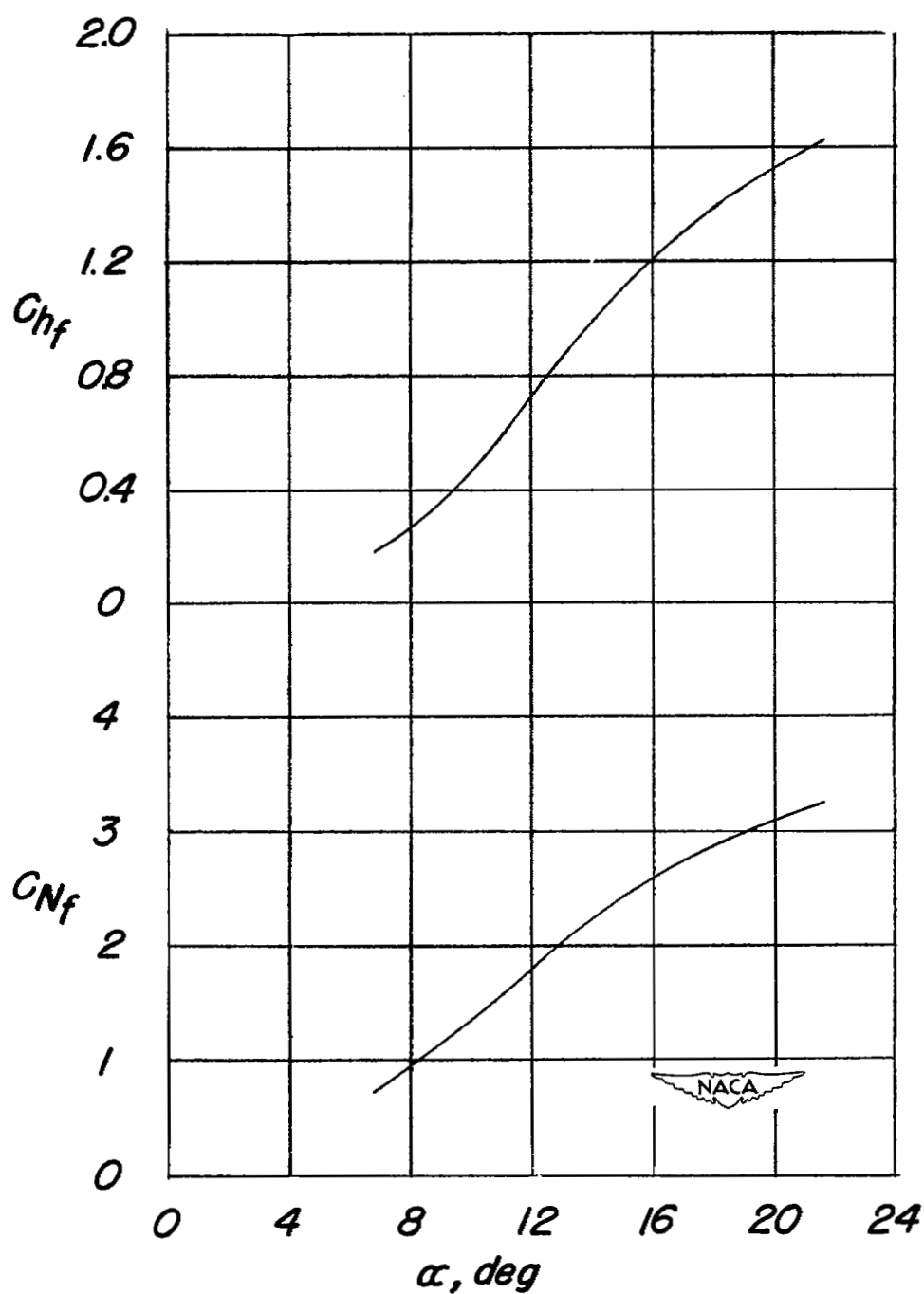


Figure 6.- Variation of total normal-force coefficient of flap and flap moment coefficient with angle of attack..

NASA Technical Library



3 1176 01436 7891